Brillouin scattering study of the phase transition in NaN_3

Toshimoto Kushida and R. W. Terhune
Scientific Research Laboratory, Ford Motor Company, P.O. Box 2053, Dearborn, Michigan 48121-2053
(Received 3 March 1986)

Brillouin scattering measurements in NaN_3 providing information on the soft acoustic modes near the trigonal-to-monoclinic phase-transition temperature T_c are reported. The soft-mode velocity in the high-temperature trigonal phase extrapolated to zero at 18 °C, 2 °C below T_c. The elastic stiffness for the soft modes varied linearly with temperatures both above and below T_c with a ratio of slopes of -2.2 ± 0.1. No line broadening in the region of the transition was observed. Sufficient measurements were made to determine all the elastic constants in the more symmetric high-temperature phase. In this phase the stiffness of the soft modes is proportional to the factor $C_{66}C_{44}$-C_{14}^2. Our measurements showed that C_{44} decreased while C_{66} and C_{14} increased, all at unusual rates, as the temperature approached T_c. It is concluded that the phase transition is ferroelastic (most likely proper ferroelastic) rather than an order-disorder transition.

I. INTRODUCTION

Sodium azide, NaN_3, undergoes a structural phase transition at about 20 °C from a high-temperature, a high-symmetry trigonal β phase with space group $R\bar{3}m$ (D_{3d}^5), to a low-temperature, low-symmetry, monoclinic α phase, with space group $C2/m$ (C_{2h}^3). This phase transition has been studied extensively by using x-ray diffraction,[1-5] specific-heat measurements,[6,7] Raman scattering,[8-11] nuclear magnetic resonance,[12,13] electron paramagnetic resonance,[14-17] and neutron diffraction.[18,19] The pressure dependence of the transition temperature,[20,21] T_c, and an anomaly in thermal expansion[21] of the bulk crystal near T_c were also studied. The observed discontinuities were so small[22] that in early studies[2] it was regarded as a second-order transition even though it was expected to be first order from Landau's theory of phase transitions.[23,24]

Since none of the elastic properties of NaN_3 were known prior to our recent observations of the acoustic soft modes in this crystal,[25] the dynamics of the phase transition for NaN_3 were not clear. Originally an order-disorder model[2] was suggested. This model invoking large displacements is the opposite limit of the ferroelastic (displacive) model where small displacements are responsible.[26] Many subsequent experimental results seemed to be in favor of the ferroelastic model.[3,27] It has been proposed that a *rotational-translational* coupling[27] produces the mode softening and subsequently the phase transition. The proposed mode-coupling mechanism[28,29] is in the same spirit as a model used to explain strongly temperature-dependent elastic properties of rubber.[30] The coupling between a lateral elastic mode of polymer chains (*translational* mode) and transverse vibrations of the molecules in the chains (*rotational* modes) is responsible for the unusual elasticity of rubber. Chihara *et al.*[31] used a similar mode-coupling concept in explaining a temperature dependence of the nuclear quadrupole resonance frequencies near the second-order phase-transition temperature in P_2Cl_{10}. This model has been used by many workers in describing the phase transition of NaN_3 and similar crystals.[32]

In this paper the experimental results of the elastic properties of NaN_3 observed with Brillouin scattering are described. Included are the details of the acoustic soft mode observations, the measured values of all the elastic constants, $C_{11}, C_{33}, C_{44}, C_{13}, C_{14}, C_{66}$ $[\equiv(C_{11}-C_{12})/2]$, and the temperature dependences of the elastic constants

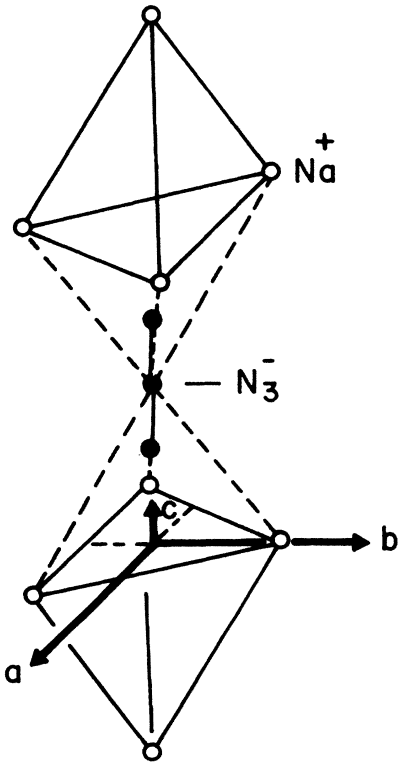

FIG. 1. An N_3^- ion and six nearest-neighbor Na^+ ions in β-NaN_3.

essential to understanding the dynamics of this phase transition.

The present results support that this phase transition is a simple proper ferroelastic transition.[33] The transition is driven by the softening of acoustic modes propagating along a few discrete directions (one dimensional softening[34]).

II. THE SOFT MODES IN NaN_3

In the trigonal (rhombohedral) β phase (Fig. 1), an azide ion N_3^-, which is a linear array, is surrounded by two Na^+ tetrahedrons. A body diagonal of Na^+ rhombohedron is defined as a c axis. A positive b direction is chosen in such a way that it is in a mirror plane containing the c axis and pointing toward Na^+. Then the a axis is defined so that the a, b, and c axis form a right-hand rectangular coordinate.[35] This convention is described by Cady.[36] The N_3^- array is along the c axis on an average in the β phase. Below T_c,[37] its average direction tilts in the b-c plane so that the ends of the array move away from one of the corners of each Na^+ triangle, and the triangles shear in the b-c plane.

The elastic stiffness tensor, $\mathbf{C}$, for the trigonal phase of NaN_3 can be written as follows:[38]

$$\mathbf{C}=\begin{bmatrix} C_{11} & C_{12} & C_{13} & C_{14} & 0 & 0 \\ C_{12} & C_{11} & C_{13} & -C_{14} & 0 & 0 \\ C_{13} & C_{13} & C_{33} & 0 & 0 & 0 \\ C_{14} & -C_{14} & 0 & C_{44} & 0 & 0 \\ 0 & 0 & 0 & 0 & C_{44} & C_{14} \\ 0 & 0 & 0 & 0 & C_{14} & C_{66} \end{bmatrix} . \tag{1}$$

The elastic free-energy (Gibbs) G is given by the tensor product,

$$G = \mathbf{AS}/2 , \tag{2}$$

where $\mathbf{S}$ is the reduced strain tensor and $\mathbf{A}$ is the stress tensor $\mathbf{CS}$.

The characteristics of the soft modes can be seen by transforming the matrices and writing as[39]

$$\mathbf{A}'=\mathbf{C}'\mathbf{S}'=\begin{bmatrix} (C_{11}+C_{12})/2 & C_{13} & 0 & 0 & 0 & 0 \\ C_{13} & C_{33}/2 & 0 & 0 & 0 & 0 \\ 0 & 0 & C_{66} & C_{14} & 0 & 0 \\ 0 & 0 & C_{14} & C_{44} & 0 & 0 \\ 0 & 0 & 0 & 0 & C_{44} & C_{14} \\ 0 & 0 & 0 & 0 & C_{14} & C_{66} \end{bmatrix} \begin{bmatrix} S_1+S_2 \\ 2^{1/2}S_3 \\ S_1-S_2 \\ S_4 \\ S_5 \\ S_6 \end{bmatrix} , \tag{3}$$

with the free energy, $G'=\mathbf{C}'\mathbf{S}'\mathbf{S}'/2=\mathbf{A}'\mathbf{S}'/2$. Soft modes are associated with small eigenvalues of $\mathbf{C}'$. Inspection of the $\mathbf{C}'$ matrix, Eq. (3), shows that the eigenvalues are doubly degenerate and a pair of eigenvalues will go to zero as the determinant of the lower 2×2 blocks goes to zero. As these eigenvalues approach zero there will be soft modes with the stiffness of the eigenvalues and a strain made up of a combination of the two strain eigenvectors. The soft modes which satisfy these conditions are described in Fig. 2 and its caption. In the experiments to be described, we concentrated on measuring the soft-mode propagating in the b-c plane at a small angle to the c axis.

III. THE EXPERIMENTAL ARRANGEMENTS

The crystals of NaN_3 were grown by slow diffusion of methanol into a saturated methanol-water solution at constant temperature (precipitation infusion method).[40] The crystals grown are thin platelets, 0.2–0.5-mm thick with 0.1–2-cm^2 faces. The crystal habits are shown in Fig. 3. An attempt to polish[11,41,42] the crystals to produce adequate faces for the Brillouin scattering experiments was not successful. A subtle damage of the crystals[7] may be responsible. The faces of the grown crystals were slightly pitted. The edges were relatively clean, however. Some blemishes and occlusions were visible. Natural crystal faces and natural or cleaved edges were used for all the measurements.

The experimental arrangements are shown in Fig. 4. The sample held by etched thin Be-Cu fingers to minimize the stress was enclosed in a copper sample holder with three windows and immersed in an index-matching liquid, acetone.[43]

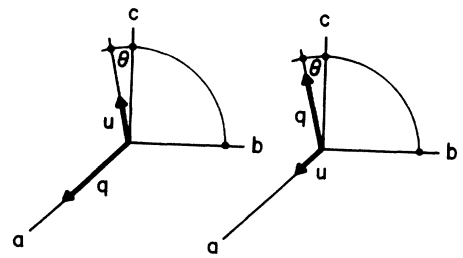

FIG. 2. Predicted propagation vectors $\vec{q}$ and displacement vector $\vec{u}$ for a pair of soft modes of NaN_3 at the transition temperature, where $C_{44}C_{66}-C_{14}^2\rightarrow0$ and $\tan\theta\rightarrow-C_{44}/C_{14}$. Both modes of the pair have the same strain. The crystal has threefold symmetry around the c axis. The other two pairs of soft modes can be found by rotating the pair shown by $\pm120°$ around the c axis.

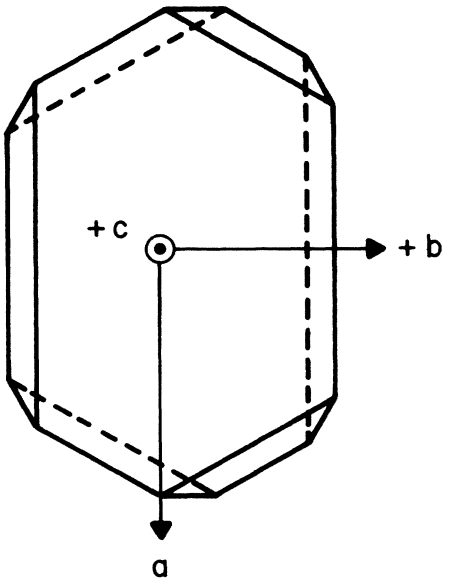

FIG. 3. Crystal habit for NaN_3 with the axes indicated. The signs are based on Cady's convention (Ref. 36).

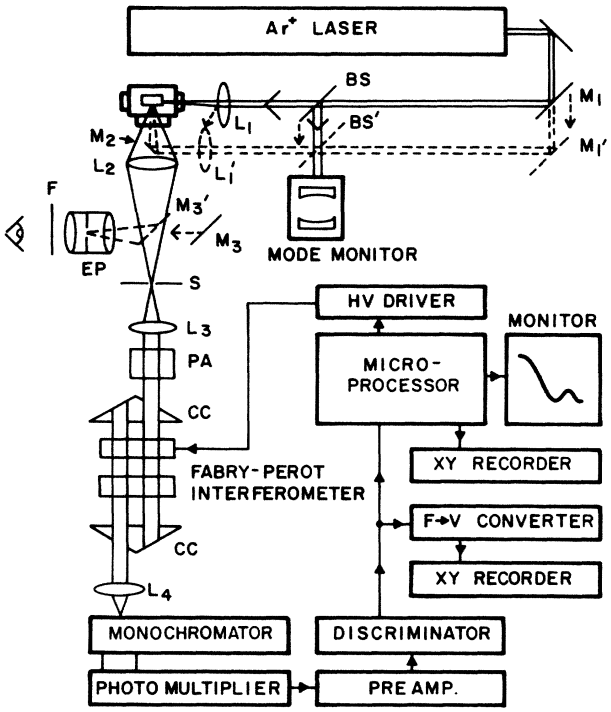

FIG. 4. A schematic of the experimental arrangement. L_1, L_2, L_3, and L_4 are the focusing and collecting lenses. M_1, M_2, and M_3 are mirrors. BS and PM are a beam splitter and a photomultiplier tube, respectively. PA is a polarization analyzer (Glan-Thompson prism). For 180° scattering measurement, M_1, BS, and L_1 were moved to the positions, M_1', BS',and L_1', respectively, and M_2 was installed.

NaN_3 is an optically uniaxial crystal with indices of refraction $n_0 = 1.368$ and $n_e = 1.720$.[44] The index of refraction of acetone is 1.359 at 20°C. The large birefringence made determining the ray directions of the incident and scattered light difficult when extraordinary rays were involved. In our measurements ordinary rays were used as much as possible. Also, when using extraordinary rays, the geometry was chosen to minimize the corrections required. Most of the measurements were made using a 90° scattering configuration. As a check on the angular corrections some measurements were made in a back scattering configuration.

The Brillouin frequency shift of the sample was calibrated against that of acetone. The temperature of the sample was measured with a thin, 130-μm diam, Fe-constantan thermocouple soldered to the sample holding finger. The thermocouple was calibrated against a certified thermometer.[45] The temperature difference between the sample and the thermocouple was checked by using another thin thermocouple embedded in a plastic dummy sample in place of the sample. The sample temperature measurement was accurate to ± 0.1 °C. The local heating[46] was estimated as less than 0.1°.

A 10—30 mW beam obtained from a single-mode coherent Ar ion laser, INNOVA 90, operating at 514.5 nm was used. When the highly temperature-dependent soft modes were studied, the laser-beam power was reduced. No dependence of the spectra on laser-beam power was observed. An adequate signal was still available since the scattering intensity increased as the reciprocal of the frequency-shift squared. Near the transition temperature the Brillouin scattering was much larger than all other scattering in the sample and was easily visible. The scattered light was collected with a macro lens, L_2.[47]

The alignment of the laser beam within the sample could be monitored using the eyepiece (EP) by moving the mirror on a motorized stage from M_3 to M_3'. Usually a filter, F, was used to remove the scattered laser radiation so that the trajectory of the beam in both the acetone and the crystal could be observed due to their fluorescence. The orientation of the sample relative to the laser beam was adjusted to within one degree by observing the crystal faces through the eyepiece.

The scattered radiation was spectrally analyzed using a microprocessor-controlled Burleigh RC 110 multipass Fabry-Perot interferometer operated in the five-pass mode. The drift in the parallelism and the spacing of the interferometer mirrors was corrected every 10 to 30 s.[48] After the alignment the microprocessor switched its function to a multichannel analyzer (MA) mode collecting the photon counts by sweeping the mirror spacing. The number of the MA channels and the dwell time on each channel were adjusted so as to collect the data most efficiently. The accumulated data was displayed on an xy recorder or stored in a tape recorder[48] for future manipulation.

A cooled RCA model C31034 photomultiplier with a GaAs photocathode with a background count rate of four photoelectrons per second was used in the photon counting mode. When studying the strong scattering from soft acoustic modes near the transition temperature the count rate was converted to a voltage with a frequency-to-

voltage converter ($F \rightarrow V$ in Fig. 4) and displayed on an xy recorder. The spectral characteristics of the laser were monitored by displaying the transmission of a scanned spherical Fabry-Perot interferometer[49] on an oscilloscope (mode monitor, Fig. 4).

Only clear crystals with well-defined faces were chosen as samples. However, many of these did not have well-defined Brillouin spectra and some showed the double spectra characteristic of twinning. Also, there was usually variability in the observed spectra for a given crystal as it was translated across the laser beam. Only regions of the crystals where the Brillouin spectrum had sharp lines with a minimum of broadband scattering and the center line intensity, mainly caused by the scattering from the crystal imperfections, was small, were used for our measurements. The quality of the spectra obtained with a given crystal deteriorated appreciably in a few hours when they were immersed in acetone. The cause of this deterioration was not determined.

IV. BRILLOUIN SPECTRA

Figures 5 and 6 show examples of the observed Brillouin spectra. The data accumulation time was 15 min. The modes are labeled by their predominant character, L for the longitudinal mode and T_1 and T_2 for the transverse modes. A weak line due to the out-of-focus scattering from the acetone mode is also visible. The frequency shifts were calibrated using the Brillouin spectrum of acetone with the sample moved out of the laser beam using an accumulation time of 2 min. The point where the spectra fold over ($\frac{1}{2}$)FSR (free spectral range), one-half the free spectral range, is indicated. The scattering geometry is indicated in the diagrams in the figures. In both cases the laser beam was polarized as an ordinary ray. A polarization analyzer, PA in Fig. 4, was removed during these runs. In Fig. 5, phonon momentum, $\vec{q}$, was along the a axis. As are shown in Fig. 6, the momentum contributing to the L and the T_1 line, $\vec{q}$, and that responsible for the depolarized T_2 line, $\vec{q}'$, had different directions in the b-c plane.

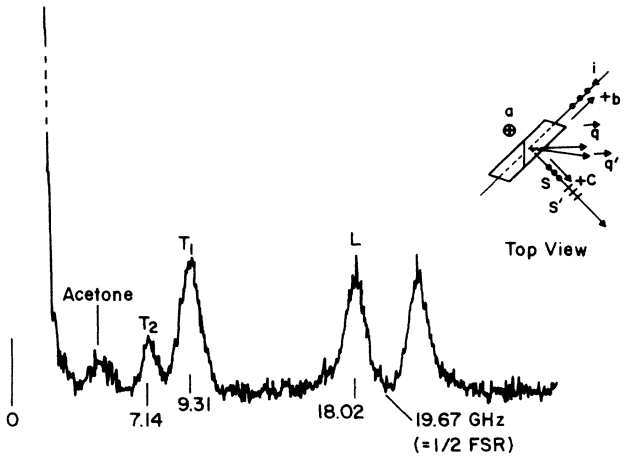

FIG. 6. Brillouin spectra of NaN_3 from the phonons propagating along 45° from the c axis in the b-c plane. The three Brillouin spectra of NaN_3, T, L_1, and L_2, are observed. A weak acetone off focus line is also shown. The incident beam is an ordinary ray. The phonon propagation direction, $\vec{q}$ observed by the ordinary scattered ray is different from $\vec{q}'$ observed by an extraordinary scattered ray.

The alignment of the crystal used to study the phonon scattering in the b-c plane which includes the soft modes near the c axis direction is shown in Fig. 7. This geometry was used for most of soft-mode studies, since the ambiguity in the birefringent correction was minimal. The scattering was observed with a 90° external angle. The sample holder was constructed so that the sample could be rotated around an axis perpendicular to the incident laser beam and the optic axis of the collecting lens L_2 in Fig. 4. The crystal was mounted with its axis along this rotation axis. The crystals were aligned using the

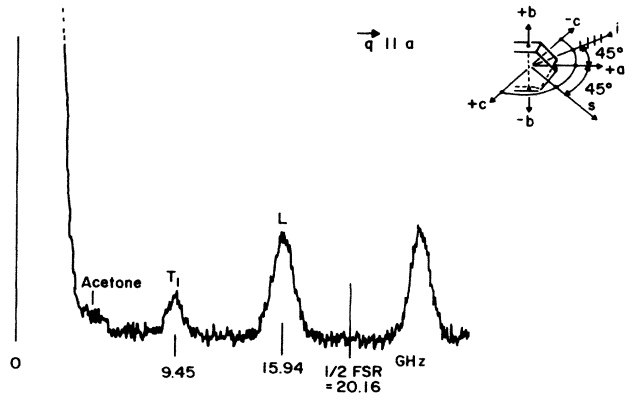

FIG. 5. Brillouin spectra from phonons propagating along the a axis. A longitudinal line, L, and one of the transverse-longitudinal line, T_1, are shown besides a weak acetone off-focus line. The directions of the incident, i, and the scattered, s, ray with respect to the crystal orientation are indicated at the top right.

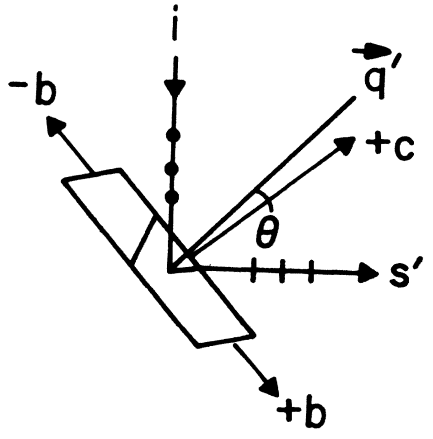

FIG. 7. The scattering geometry for observing the phonon scattering in the b-c plane which includes the soft mode near the c axis direction. The incident beam, i, was an ordinary ray, whereas only a scattered extraordinary ray, s', was observed by filtering out the polarized ray with a polarization analyzer (PA in Fig. 4).

eyepiece, EP, and the lens, L_2, as a microscope observing the edges defined by the intersection of the crystal faces.

The determination of the origin of the rotation angle, defined as the angle where the a-b plane is parallel to the incident beam, turned out not to be trivial. The alignment using a most obvious method, i.e., to use the retroreflection of the crystal face, was not practical, since the reflected light was spread over a large angle with uneven brightness due to the pitting of the surface. The next obvious alignment method using a telescope is to align the a-b plane parallel to the observing direction, where this direction has been adjusted parallel to the beam. This method was also not satisfactory due to the shallow depth of focus in the present telescope arrangement. Another obvious method is to shine the laser beam to the a-b plane near the grazing angle and try to find the angle where the beam is exactly in the a-b plane. The accuracy achieved was only several degrees due to the roughness of the a-b face. The precise alignment was obtained by using well-defined edges of the crystal rather than the surface as follows: a small mirror was installed temporarily below the crystal. Both the incident beam and the edges of the crystal were observed in the eyepiece through this *look-up* mirror. The sample was rotated until both were parallel. The mirror was removed after the alignment.

Figure 8 shows the observed angular dependence of the frequency of the lowest-frequency transverse mode. Near T_c the frequency was a minimum for phonons propagating at $-10.7°$ from the c axis. The laser was polarized as an ordinary ray and the scattered light as an extraordinary ray. Since the two rays have different indices the momentum transferred to the phonons did not bisect the external incident and scattering directions. The calculated angle[50–55] between the phonon propagation direction and the c axis rather than the rotation angle of the crystal has been plotted. The correction near the minimum was approximately 0.5°. The linewidth was sharpest and the peak intensity strongest near the minimum. This could be explained if the lines were inhomogeneously broadened due to small angle variations in the c axis direction within the crystal as noticed by Schmidt.[16]

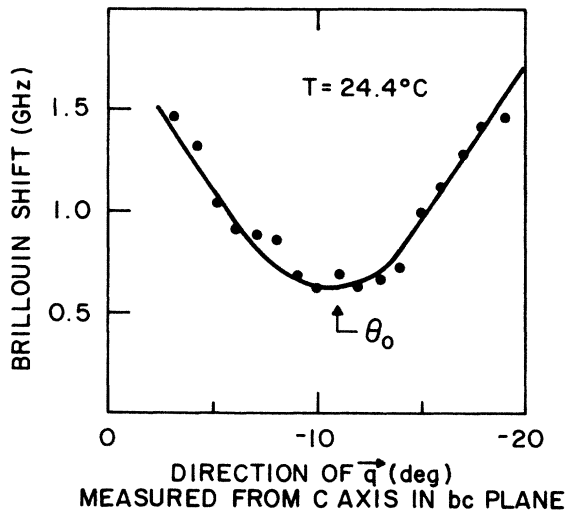

FIG. 8. The Brillouin shift from the low-frequency mode as a function of angle for the scattering phonon direction. The phonon propagation vector, $\vec{q}$, is in the b-c plane. The angle is measured from the c axis.

Figure 9 shows the spectra of the low-frequency mode observed as a function of temperature with θ_0 of $-10.7°$ The sharp dependence of frequency on temperature is apparent. The intensity of the scattering was large enough that the photon count rate was recorded directly on an xy recorder using a frequency-to-voltage converter as shown in Fig. 4. The sample container was sealed with an In O-ring to prevent boiling of the acetone as the temperature was raised. The sample holder was insulated with a vacuum jacket and the temperature was controlled using an electric heater or dry-ice-cooled nitrogen gas flow.

Studies of the spectra of the soft modes were also made at a lower temperature through T_c by reducing the temperature at rates near 0.2 °C per min (Fig. 10). At the transition temperature, T_c, a marked increase in the elas-

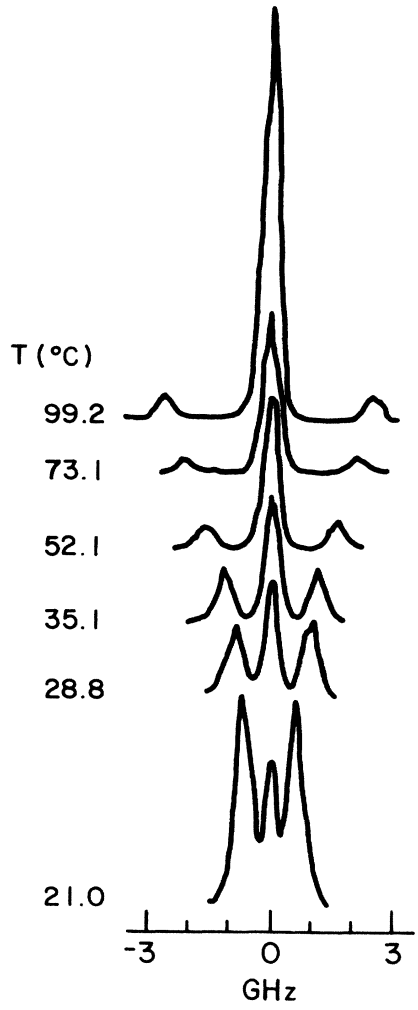

FIG. 9. Observed soft-mode Brillouin spectra as a function of temperature. The direction of the participating soft-mode is off by $-10.7°$ from the c axis in the b-c plane. The count rate of the scattered photons was converted to a voltage and recorded on an x-y recorder without signal accumulation.

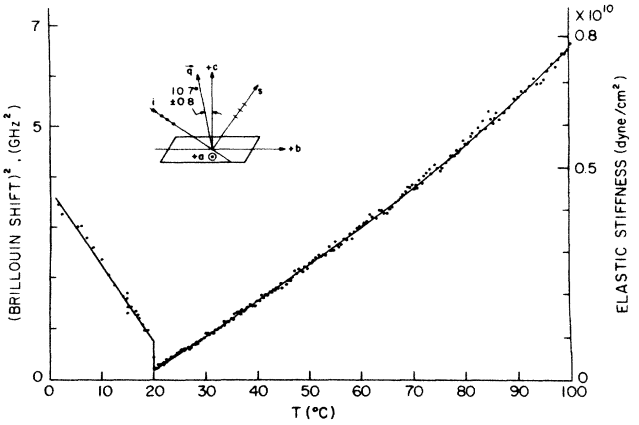

FIG. 10. Elastic stiffness for the soft acoustic mode in NaN_3 as a function of temperature. The square of the observed Brillouin shift is also shown. The propagation direction of the soft mode is indicated at the top.

tic scattering peak occurred over times of the order of half a minute. This increase is believed to be due to the formation of multiple domains of the lower symmetry phase with different orientations.[56] When the sample was viewed through the eyepiece, the brightness of the sample was not uniform suggesting that the density of domain walls was related to sample imperfections. Regions with reduced elastic scattering were chosen to make our measurements on the Brillouin scattering below T_c.

V. ANALYSIS AND ELASTIC CONSTANTS MEASUREMENTS

Considering acoustic wave propagation in a direction $\vec{q}$, one obtains the following equation (Christoffel equation),[57,58] for the eigenelastic stiffness C_s corresponding to each of three modes.

$$\begin{vmatrix} \lambda_{11}-C_s & \lambda_{12} & \lambda_{13} \\ \lambda_{12} & \lambda_{22}-C_s & \lambda_{23} \\ \lambda_{13} & \lambda_{23} & \lambda_{33}-C_s \end{vmatrix} = 0 , \tag{4}$$

where

$$\lambda_{ij} = l^2 C_{1i1j} + m^2 C_{2i2j} + n^2 C_{3i3j} + lm(C_{1i2j} + C_{2i1j}) + ln(C_{1i3j} + C_{3i1j}) + mn(C_{2i3j} + C_{3i2j}) .$$

Here C_{ijkl} are components of the elastic stiffness tensor, and l, m, and n are the direction cosines for $\vec{q}$. The velocity of each acoustic wave, V_P, is related to the eigen stiffness, C_s by,

$$\rho V_P^2 = C_s , \tag{5}$$

where ρ is the density of the crystal. The equation for λ_{ij}, Eq. (4), can be written in terms of the reduced elastic stiffness tensor components C_{pq} $(p,q = 1,2,\ldots,6)$ by replacing the first two indices of C_{ijkl} with p and the last two with q.

For $\vec{q}$ along the a axis one obtains

$$\begin{vmatrix} C_{11}-C_s & 0 & 0 \\ 0 & C_{66}-C_s & C_{14} \\ 0 & C_{14} & C_{44}-C_s \end{vmatrix} = 0 . \tag{6}$$

One obtains for $\vec{q}$ in the b-c plane

$$\begin{vmatrix} \lambda_{11}-C_s & 0 & 0 \\ 0 & \lambda_{22}-C_s & \lambda_{23} \\ 0 & \lambda_{23} & \lambda_{33}-C_s \end{vmatrix} = 0 , \tag{7}$$

with

$$\lambda_{11} = C_{66}\sin^2\theta + C_{44}\cos^2\theta + 2C_{14}\sin\theta\cos\theta ,$$
$$\lambda_{23} = -C_{14}\sin^2\theta + (C_{44}+C_{13})\sin\theta\cos\theta ,$$
$$\lambda_{22} = C_{11}\sin^2\theta + C_{44}\cos^2\theta - 2C_{14}\sin\theta\cos\theta ,$$
$$\lambda_{33} = C_{44}\sin^2\theta + C_{33}\cos^2\theta .$$

Here θ is the angle measured from the c axis.

An uncoupled mode in Eq. (7), $\lambda_{11}-C_s=0$, becomes one of the soft modes[25] when θ is chosen so as to minimize C_s.

The minimum in C_s, C_{s0}, occurs for $\theta=\theta_0$ given by[25,59]

$$\tan(2\theta_0) = -2C_{14}/(C_{66}-C_{44}) , \tag{8}$$

with

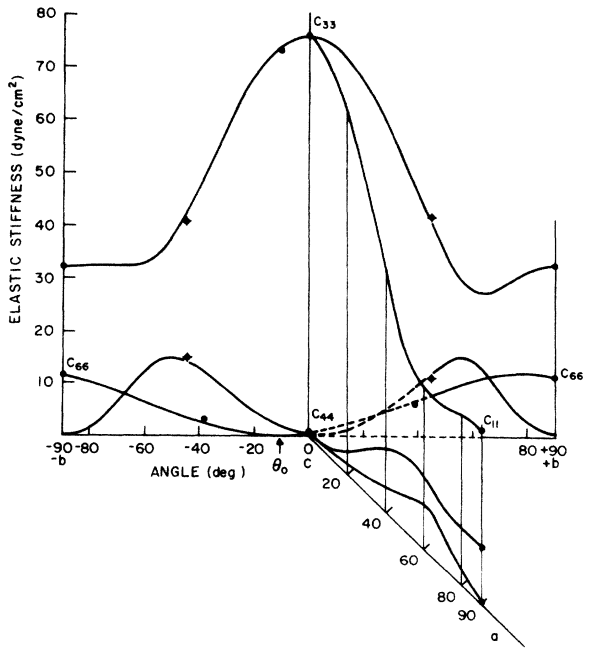

FIG. 11. Elastic stiffness as a function of the propagation direction of the phonons. The dots are the measured values. The curves were calculated using Eq. (4) with the derived elastic constants shown in Table I. The elastic constants associated with "pure" modes, C_{11}, C_{33}, C_{44}, and $C_{66}=(\frac{1}{2})(C_{11}-C_{12})$, are indicated.

TABLE I. The elastic constants and their temperature dependence of NaN_3. θ_0 is one of the soft-mode directions as measured from the c axis in the b-c plane. Another soft mode is along the a axis direction.

$C_{11}=32.4\pm0.8$, $C_{44}=0.45\pm0.02$[a]	
$C_{33}=75.5\pm0.6$, $C_{66}=10.5\pm0.2$[a]	
$C_{13}=17.6\pm3.5$, $C_{14}=2.0\pm0.1$[a]	
$dC_{66}/dT=-0.015\pm0.014$[b]	$d\ln C_{66}/dT=-0.0014$[c]
$dC_{14}/dT=-0.0078\pm0.003$[b]	$d\ln C_{14}/dT=-0.0038$[c]
$dC_{44}/dT=+0.005\pm0.0005$[b]	$d\ln C_{44}/dT=+0.0110$[c]
	$d\ln C_{11}/dT=-0.0001$[c]
$\theta_0=-10.7°\pm0.8$	

[a] $\times 10^{10}$ dyn/cm^2, 25 °C.
[b] $\times 10^{10}$ dyn/cm^2/deg.
[c] deg^{-1}.

$$C_{s0}=C_{44}(C_{66}C_{44}-C_{14}^2)/(C_{14}^2+C_{44}^2)\ . \tag{9}$$

When C_{s0} is small, Eqs. (8) and (9) reduce to

$$\tan\theta_0=-C_{44}/C_{14}\ , \tag{8'}$$

and

$$C_{s0}=(C_{66}C_{44}-C_{14}^2)/(C_{66}+C_{44})\ . \tag{9'}$$

The values for C_{11}, C_{66}, C_{33}, and C_{44} were determined from the spectra observed with the acoustic modes propagating along the following directions:[35,59] C_{11}, $\vec{q}\,||\hat{a}$; C_{66}, $q||\hat{b}$; and C_{33} and C_{44}; $\vec{q}\,||\hat{c}$. The value of C_{14} was determined from the θ dependence of C_s for the uncoupled mode in Eq. (7). Finally, from the measurements with $\theta=\pm45°$, C_{13} was obtained by the stiffness obtained by diagonalizing the lower block in Eq. (7),[60]

$$2C_s=(C_{11}+C_{33})/2+C_{44}\mp C_{14}+\{[(C_{11}-C_{33})/2\mp C_{14}]^2+(C_{44}+C_{13}\mp C_{14})^2\}^{1/2}\ .$$

The elastic constants thus obtained are shown in Table I. Using these C_{ij}'s, the C_s curves were calculated for $\vec{q}$ in the b-c plane and in the a-c plane (Fig. 11). The curves are symmetric in the a-c plane with respect to the c axis, but asymmetric in the b-c plane. The C_s values for $\vec{q}$ in the a-b plane are virtually angular independent.[24]

The temperature dependence of some of the stiffness constants are also shown in Table I. An anomalous thermoelasticity in C_{44}, C_{66}, and C_{14} is believed to be responsible for the mode softening.[61] The temperature dependence of these stiffness constants were obtained as follows: From Eq. (7) dC_s/dT of the uncoupled mode is given for small angle θ ($\lesssim 10°$) as

$$dC_s/dT=dC_{44}/dT+2\theta(dC_{14}/dT)+\theta^2 \text{ term}\ . \tag{10}$$

The values dC_s/dT derived from the observed temperature dependence of the Brillouin shift squared in Fig. 12 are plotted as a function of θ in Fig. 13. Because of relatively large experimental errors, the θ^2 term in Eq. (10) was neglected. The slope of the straight line and the intercept at $\theta=0$ give $2dC_{14}/dT$ and dC_{44}/dT, respectively. dC_{66}/dT was measured from the mode for $\vec{q}\,||\hat{b}$. The results are shown in Table I. For a comparison, $d\ln C_{11}/dT$ was also measured from the mode for $\vec{q}\,||\hat{a}$.

The expected anomaly in the thermoelasticity is noted for C_{44}, C_{14}, and C_{66}. C_{44} softens by a large amount ($d\ln C_{44}/dT=1.1\%$/deg), but C_{66} and C_{14} somewhat harden with decreasing temperature.[62,63] The fractional change in these elastic constants are much larger than that of C_{11}. The temperature dependence of the soft mode for small C_{s0} is from Eq. (9),

$$d(C_{44}C_{66}-C_{14}^2)/dT=C_{44}C_{66}(d\ln C_{44}/dT+d\ln C_{66}/dT)-C_{14}^2(2d\ln C_{14}/dT)\ .$$

Near T_c, $d\ln C_{44}/dT$ (≈0.01) and $-2d\ln C_{14}/dT$ (≈0.008) contribute approximately the same amount to the mode softening while the term $d\ln C_{66}/dT$ can be neglected.

It has been shown[39,64] that a pair of complementary soft modes exist near the ferroelastic transition; the second of the pair is the one where $\vec{q}$ and $\vec{u}$, particle velocity, are interchanged in the first one. The second mode was found in this sample for $\vec{q}\,||\hat{a}$,[25,65] whose elastic stiffness,

$$C_s=(\tfrac{1}{2})\{C_{66}+C_{44}-[(C_{66}-C_{44})^2+4C_{14}^2]^{1/2}\}\ ,$$

asymptotically becomes the same value as that of the first soft mode, Eq. (9'), as $C_{44}C_{66}\to C_{14}^2$.

VI. DISCUSSION

Since Pringle and Noakes[2] proposed the order-disorder model, a great deal of controversy persisted as to the nature of the phase transition in NaN_3.[27,62] This model be-

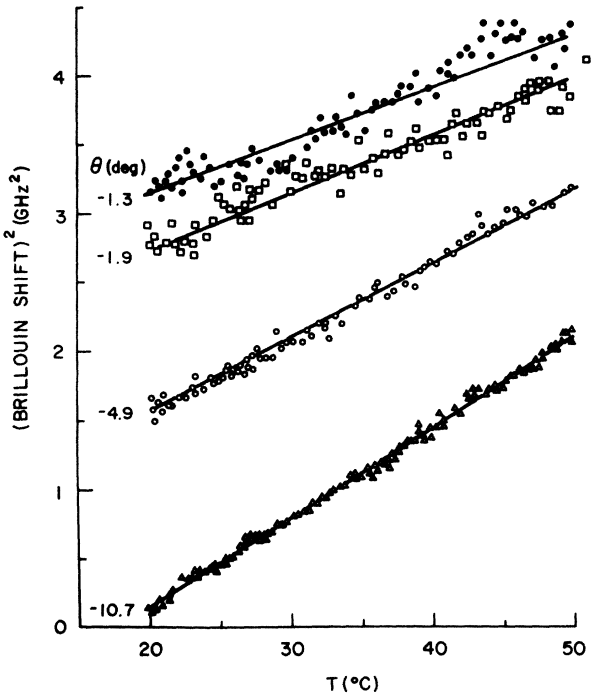

FIG. 12. The temperature dependence of the (Brillouin shift)^2 from the low-frequency mode as a function of angle, θ, from the c axis in the b-c plane.

came gradually disfavored, because of a very small specific heat anomaly at 1_c (Ref. 6) and absence of anomaly in the nuclear spin-lattice relaxation time, T_1, near T_c.[13] There is no indication of Arrhenius type temperature dependence in the T_1 data normally observed when there is a molecular reorientation.

Another model for the distortive structure phase transition was proposed.[3,13] A displacive (ferroelastic) model is an opposite limiting case to the order-disorder one.[26,66] Meanwhile, the absence of the soft-mode observation usually associated with this model troubled many workers.[67] A somewhat vague intermediate model called "dynamic order-disorder" picture was suggested.[10,19] An erroneous prediction that NaN_3 has no soft acoustic mode[27,68] might have added an additional confusion.

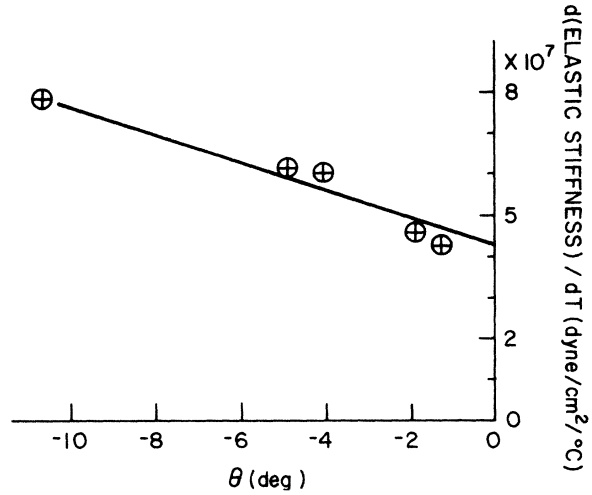

FIG. 13. The temperature dependence of the elastic stiffness as a function of angle measured from the c axis in the b-c plane derived from the curves shown in Fig. 11.

In Landau's (Gibbs) free-energy expansion in terms of an order parameter Q[23],

$$G = G_0 + (1/2)a(T - T_c)Q^2 + (\tfrac{1}{3})bQ^3 + (\tfrac{1}{4})cQ^4 + \ldots , \quad (11)$$

where $a(\geq 0)$, $b(\geq 0)$, and $c(>0)$ are constants. If Q is proportional to a spontaneous strain responsible to the phase transition, it can be shown that the slope ratio, $(dC_s/dT)_\alpha/(dC_s/dT)_\beta$ is -2, if b is small.[69] Such a transition is termed a proper ferroelastic transition in which $a(T - T_c)$ and $-2a(T - T_c)$ are the elastic stiffness of the soft mode for high- and low-temperature phase, respectively. And the soft-mode strain would be an order parameter for the transition. The same conclusion would be reached in a material such as NaN_3 where a two-component order parameter is involved.[70] However, the soft-mode strain in the high-symmetry phase of NaN_3 cannot be used as a primary order parameter for the phase transition. The symmetry of the changes which takes place at the phase transition does not match the symmetry of the strains associated with the soft modes.[33] For this to be true the soft modes would have to travel along the c axis. Nevertheless the observed ratio -2.2 ± 0.1 for the NaN_3 transition would seem to support the use of the above transition model.[71,72]

Schwabl and coworkers[34,73,74] showed that in the proper ferroelastic transitions, if the acoustic modes soften in certain discrete directions, Landau's theory based on a mean-field concept is valid, and the critical behavior is classical. This is consistent with the present observations where the width of the Brillouin lines is temperature independent and no deviation from classical critical exponents for the sound velocity was observed near T_c.

Landau's analysis indicates that a third-order term in the free-energy expansion in terms of the order parameter is allowed for the NaN_3 transition. The presence of such a term would make the transition a first-order transition.[75] Yet most of the experiments indicate the transition being almost completely continuous.[6,8,10,14] Some evidences of the discontinuity were found recently. Midorikawa *et al.*[21] observed a small discontinuity in thermal expansion and also noticed a distinct phase front under a polarization microscope. Aghdaee and Rae[3] observed a small discontinuity in a strain component e_{13} at T_c. Hirotsu *et al.*[7] noticed a very small thermal hysteresis (0.03°) in their specific-heat measurements near T_c. They declined to claim this as evidence of the first-order nature of the transition, however. It is striking[76] to notice that NaN_3 displays discontinuities of similar to or even smaller than that of the materials whose third-order terms in the free-energy expansion vanish due to symmetry relations.[77]

The observed residue of the elastic stiffness at T_c, 2.2×10^8 dyn cm^{-2}, seems to be slightly dependent on the quality of the crystals. The residue is not limited by the misalignments of the crystals, however. The Brillouin

shift is not sensitive to the misalignment of less than one degree as long as they are aligned close to the minimum shift direction (Fig. 8). The observed distinct discontinuity in the stiffness at T_c is not necessarily associated with the first-order nature of the transition. A small discontinuity in the compressibility is expected even for a perfect second order phase transition.[78]

It can be said that the small discontinuity in the stiffness and its residue at T_c are not inconsistent with the very weak first-order nature of this phase transition.

ACKNOWLEDGMENTS

One of the authors, T.K. would like to thank Professor S. D. Mahanti, Professor Yoshihiro Ishibashi, and Dr. D. Sahu for helpful discussions.

[1]S. B. Hendricks and L. Pauling, J. Am. Chem. Soc. **47**, 2904 (1925).

[2]G. E. Pringle and D. E. Noakes, Acta Crystallogr. **B24**, 262 (1968).

[3]S. R. Aghdaee and A. I. M. Rae, J. Chem. Phys. **79**, 4558 (1983).

[4]E. D. Stevens and H. Hope, Acta Crystallogr. **A33**, 723 (1977).

[5]R. B. Parsons and A. D. Yoffe, Acta Crystallogr. **20**, 36 (1966).

[6]R. W. Carling and E. F. Westrum, Jr., J. Chem. Thermodyn. **8**, 565 (1976).

[7]S. Hirotsu, M. Miyamota, and K. Ema, J. Phys. C **16**, L661 (1983).

[8]Z. Iqbal and C. W. Christoe, Solid State Commun. **17**, 71 (1974).

[9]Zafar Iqbal and C. W. Christoe, Chem. Phys. Lett. **29**, 623 (1974).

[10]Zafar Iqbal, J. Chem. Phys. **59**, 1769 (1973).

[11]George J. Simonis and C. E. Hathaway, Phys. Rev. B **10**, 4419 (1974).

[12]I. D. Campbell and C. K. Coogan, J. Chem. Phys. **44**, 2075 (1966).

[13]Kenneth R. Jeffrey, J. Chem. Phys. **66**, 4677 (1977).

[14]B. S. Miller and G. J. King, J. Chem. Phys. **39**, 2779 (1963).

[15]F. J. Owens, Chem. Phys. Lett. **35**, 269 (1975).

[16]Werner W. Schmidt, Z. Phys. B **46**, 17 (1982).

[17]Werner W. Schmidt and Albrecht Wieser, Z. Phys. B **52**, 237 (1983).

[18]Hamid A. Rafizadeh, Sidney Yip, and Henry Prask, J. Chem. Phys. **56**, 5377 (1972).

[19]C. S. Choi and E. Prince, J. Chem. Phys. **64**, 4510 (1976).

[20]C. E. Weir, S. Block, and G. J. Piermarini, J. Chem. Phys. **53**, 4265 (1970).

[21]Michio Midorikawa, Hiroshi Orihara, Yoshihiro Ishibashi, Tadaharu Minato, and Hikaru Terauchi, J. Phys. Soc. Jpn. **52**, 3833 (1983).

[22]For example, a specific-heat anomaly at T_c is very small, Ref. 6.

[23]L. D. L. Landau and E. M. Lifshitz, *Statistical Physics* (Pergamon, London, 1958), p. 434.

[24]A similar transition has been observed in *sym*-triazine, which undergoes a trigonal-to-monoclinic transition. For example, A. Yoshihara, C. L. Pan, E. R. Bernstein, and J. C. Raich, J. Chem. Phys. **76**, 3218 (1982). Its phase transition turned out to be of weak first order. It does not seem to be well understood why the first-order nature of this transition is so weak for these classes of crystals. Another class of materials having a very subtle first-order transition, seemingly violating the Landau's criterion, are some of *A*15 superconductors, V_3Si and Nb_3Sn. The transition is from cubic to tetragonal, however, J. Wanagel and B. W. Batterman, J. Appl. Phys. **41**, 3610 (1970). I. R. Testardi and T. B. Bateman, Phys. Rev. **154**, 402 (1967). H. R. Ott, B. S. Chandrasekhar, and B. Seeber, Phys. Rev. B **31**, 2700 (1985).

[25]Toshimoto Kushida and R. W. Terhune, Phys. Rev. B **30**, 3554 (1984).

[26]A. D. Bruce and R. A. Cowley, *Structural Phase Transitions* (Taylor and Francis, London, 1981), p. 3 or Adv. Phys. **29**, 219 (1980).

[27]J. C. Raich and Hüller, J. Chem. Phys. **70**, 3669 (1979).

[28]K. H. Michel and J. Naudts, Phys. Rev. Lett. **39**, 212 (1977); J. Chem. Phys. **67**, 547 (1977).

[20]D. Sahu and S. D. Mahanti, Phys. Rev. B **26**, 2981 (1982).

[30]For example, L. R. G. Treloar, *The Physics of Rubber Elasticity*, 3rd ed. (Clarendon, Oxford, 1975), p. 24.

[31]Hideaki Chihara, Nobuo Nakamura, and Masashi Tachiki, J. Chem. Phys. **59**, 5387 (1973).

[32]NaN_3; Refs. 3 and 8, TlN_3; Ref. 9, *sym*-triazine; A. I. M. Rae, J. Phys. C **15**, 1883 (1982).

[33]Kêitsiro Aizu, J. Phys. Soc. Jpn. **28**, 706 (1970).

[34]F. Schwabl, Ferroelectrics **24**, 171 (1980) and private communication.

[35]Yakov Eckstein, A. W. Lawson, and Darrell H. Reneker, J. Appl. Phys. **31**, 1534 (1960).

[36]W. G. Cady, *Piezoelectricity* (McGraw-Hill, New York, 1946), p. 23.

[37]T_c determined by the specific-heat measurements: 293.0±0.1 K, Ref. 6; 19.80±0.05 °C, Ref. 7; 292.2 K quoted in Ref. 3.

[38]For instance, J. F. Nye, *Physical Properties of Crystals*, (Oxford, London, 1957), p. 141.

[39]R. W. Terhune, Toshimoto Kushida, and G. W. Ford, Phys. Rev. B **32**, 8416 (1985).

[40]T. A. Richter and O. Haase, Mater. Res. Bull. **5**, 511 (1970).

[41]James I. Bryant, J. Chem. Phys. **40**, 3195 (1964).

[42]R. W. Dreyfus and P. W. Levy, Proc. R. Soc. London, Ser. A **246**, 233 (1958).

[43]Acetone was dryed with molecular sieve, (8-12 Mesh), activated Type 5A.

[44]T. J. Lewis, Trans. Faraday Soc. **62**, 889 (1966).

[45]A certified grade thermometer which has been calibrated against an NBS standard thermometer, Fisher Scientific Co.

[46]When the laser beam struck a rough spot on the sample, however, large local heating was noticed by bubble formation in acetone.

[47]MICRO NIKKOR, *F* 2.8, 55 mm, operated at an effective *F* number of 3.4.

[48]Thomas H. Wood, Rev. Sci. Instrum. **49**, 790 (1978). The present system consists of a home-assembled INTEL microprocessor 8080 CPU (central processing unit) programmed in an assembly language with a TEKTRONIX 4923 tape recorder as a program and a data storage.

[49]TROPEL (Now COHERENT), Model 240.

[50]R. W. Dixon, IEEE J. Quantum Electron. **QE-3**, 85 (1967).

[51]Lawrence L. Hope, Phys. Rev. **166**, 883 (1968).

[52]D. Keller and C. Søndergaard, Jpn. J. Appl. Phys. **13**, 1765

(1974).
[53]Ole Keller, Phys. Rev. B **11**, 5059 (1975).
[54]R. Vacher, L. Boyer, and M. Boissier, Phys. Rev. B **6**, 674 (1972).
[55]R. Vacher and L. Boyer, Phys. Rev. B **6**, 639 (1972).
[56]J. Sapriel, Phys. Rev. B **12**, 5128 (1975).
[57]Warren P. Mason, *Physical Acoustics, I Part A,* (Academic, New York, 1964), p. 325.
[58]Walter G. Mayer and Paul M. Parker, Acta Crystallogr. **14**, 725 (1961).
[59]K. Brugger, J. Appl. Phys. **36**, 759 (1965), Laue group RI.
[60]Equations (14) and (12) in Ref. 35.
[61]J. C. Raich and E. R. Bernstein, J. Chem. Phys. **73**, 1955 (1980).
[62]J. C. Raich and N. S. Gillis, J. Chem. Phys. **65**, 2088 (1976).
[63]For *sym*-triazine, however, Raich and Bernstein predicted that C_{44} as well as C_{14} and C_{66} would soften as $T \rightarrow T_c$, Ref. 61.
[64]S. Aubry and R. Pick, J. Phys. **32**, 657 (1971).
[65]In benzil, the two soft modes were shown in the numerical calculation of C_s, R. Vacher, M. Boissier, and J. Sapiel, Phys. Rev. B **23**, 215 (1981), Fig. 2. A neutron diffraction study of *sym*-triazine indicated the mode softens in the *a* and the *c* direction. The latter mode could have been slightly off from the *c* axis. I. U. Heilmam, W. D. Ellenson, and J. Eckert, J. Phys. **12**, L185 (1979). Benzil and *sym*-triazine have the similar crystal structure as that of NaN_3.
[66]Walther Rehwald, Adv. Phys. **22**, 721 (1973).
[67]For example, see George J. Simonis and C. E. Hathaway, Ref. 11.
[68]R. A. Cowley, Phys. Rev. B **13**, 4877 (1976).
[69]For example, see A. D. Bruce and R. A. Cowley, Structural Phase Transitions, Ref. 26, p. 41, Eq. (I.4.6).
[70]A. D. Bruce and R. A. Cowley, *Structural Phase Transitions,* Ref. 26, p. 52.
[71]Jean-Claude Tolèdano and Pierre Tolèdano, Phys. Rev. B **21**, 1139 (1980). Tolèdano *et al.*, however, classified NaN_3 as a pseudo proper ferroelastic in their later paper. P. Tolèdano, M. M. Fejer, and B. A. Auld, Phys. Rev. B **27**, 5717 (1983). The point-group change in their Table I for NaN_3 is incorrect.
[72]A. D. Bruce and R. A. Cowley, *Structural Phase Transitions,* Ref. 26, p. 42.
[73]R. Folk, H. Iro, and F. Schwabl, Phys. Lett. **57A**, 112 (1976).
[74]R. Folk, H. Iro, and F. Schwabl, Phys. Rev. B **20**, 1229 (1979).
[75]George Simonis and C. E. Hathaway, Ref. 11, Table III.
[76]Ref. 71, another example is *sym*-triazine which has a similar crystal structure. Other examples with different crystal structure are V_3Si and Nb_3Sn, Ref. 24.
[77]For example, a minimum Brillouin shift observed at T_c for $BiVO_4$, which complies the Landau's criterion, is almost one order of magnitude larger than the residual shift in NaN_3. Gu Benyuan, M. Copic, and H. Z. Cummins, Phys Rev. B **24**, 4098 (1981).
[78]L. D. L. Landau and E. M. Lifshitz, Statistical Physics, Ref. 23, p. 438.